Slope Instability Below Historic Mine Benches in the Northern Coalfields of West Virginia

MUHAMMAD ALI
AARON E. MAXWELL*

Department of Geology and Geography, West Virginia University, Morgantown, WV 26505

CHARLES M. SHOBE

U.S. Forest Service, Rocky Mountain Research Station, Fort Collins, CO 80526

SARAH FARHADPOUR

Department of Geology and Geography, West Virginia University, Morgantown, WV 26505

Key Terms: ***Slope Stability, Landslides, Surface Coal Mining, Mine Bench, Mine Reclamation, Geohazards***

ABSTRACT

Anthropogenic reshaping of landscapes can increase landslide activity. One example of heavily modified, landslide-prone landscapes is the Appalachian region, which hosts weak geologic strata, steep slopes, a humid climate, geologically recent river incision, and large-scale landscape modifications resulting from surface mining. Surface mining conducted before the Surface Mine Control and Reclamation Act (SMCRA) of 1977 did not require reclamation to approximate original contour, so remnant highwalls and mine benches are common throughout Appalachia. This study investigated the occurrence of slope instability and failure beneath pre-law mine benches in the northern coalfields of West Virginia. Mine bench features were manually digitized based on interpretation of high-spatial-resolution digital terrain data and aerial orthophotography, and ancillary geospatial data (i.e., mine permit boundary and disturbance extent data sets). A subset of mine bench features, stratified by coal seam, was randomly selected for slope stability analysis. The lower margins of the randomly selected mine benches were differentiated into segments with and without evidence of slope failure or instability. Results suggest that local topographic slope and aspect were not strong determinants of slope instability beneath mine benches. However, the coal seam or unit that was mined was an important determining factor. The Pittsburgh seam, and to a lesser extent the Redstone seam, had a larger proportion of their lower margins showing evidence of slope failure than did other seams. This study highlights that local-scale geology controls the geomorphic response to human landscape modifications and suggests that proactive reclamation of surface coal mines might reduce slope-failure geohazards.

INTRODUCTION

Humans, Earth's primary agents of geomorphic change (Hooke, 2000; Wilkinson, 2005), reshape landscapes in ways that increase the potential for geohazards, including hillslope failures (Froude and Petley, 2018). Because landslide geohazards in human-modified landscapes are the product of both natural physiography and an effectively infinite array of human choices, predictive power over landslide occurrence in such landscapes remains elusive.

Surface mining is one of the most significant ways in which humans alter landscapes and the potential for landsliding (Reed and Kite, 2020). Mining displaces large amounts of material and often increases the total volume of sediment in a landscape by transforming bedrock into piles of waste rock fragments with significant porosity (Zipper and Skousen, 2021). Waste rock deposits have been shown to be less erosion resistant than the surface material of the pre-mining landscape (e.g., Reed and Kite, 2020; Bower et al., 2024; and Shobe et al., 2024). However, the specific causal factors governing the risk of post-mining hillslope failure are uncertain. Here, we document slope instability below mine benches in the northern coalfields of West Virginia, in the Appalachian region of the United States, to determine controls on post-mining landsliding. Although failures may also occur upslope of highwalls and mine benches, features that are described below and visualized in Figures 1

*Corresponding author email: Aaron.Maxwell@mail.wvu.edu

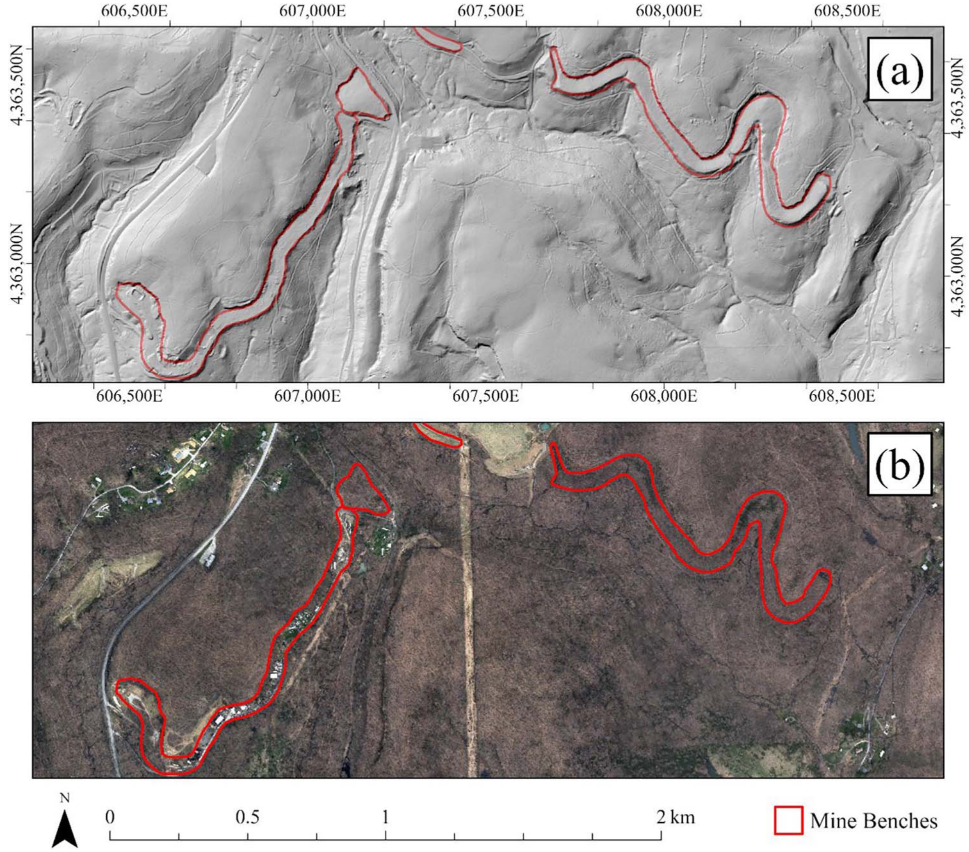

Figure 1. Example mine benches in Preston County, WV. Bench features were manually digitized by the researchers. (a) Image represents the bare earth surface as a hillshade model created from a lidar-derived digital terrain model. (b) Image shows the same extent in leaf-off aerial orthophotography. Imagery and lidar data were provided by the West Virginia GIS Technical Center (WVGISTC). The North American Datum 1983 (NAD83) Universal Transverse Mercator (UTM) Zone 17N coordinate system is used.

through 3, we focused on downslope failures because (1) displaced materials were most commonly placed downslope of the mine bench, whereas slopes above the highwall and bench were not commonly modified by mining, and (2) mechanisms and causes of downslope and upslope failures may differ.

The terrain of the northern coalfields of West Virginia is landslide-prone even before considering human alterations. Regional topography is characterized by a dissected plateau with steep slopes and a high degree of local topographic variability (Strausbaugh and Core, 1978). Due to these locally steep slopes and other factors, including a humid climate, heavy precipitation events, and weak geologic strata, this region is prone to landslides and other forms of slope failures (Coates, 1977; Southworth, 1988; and Wooten et al., 2016). These geohazards have detrimental effects on personal property, infrastructure, and local economies (U.S. Geological Survey, 2024). Thus, it is important to characterize slope failure risks and contributing factors.

The northern coalfields have also been heavily modified by historic resource extraction, specifically underground and surface coal mining (Zipper et al., 1989, 2011). Before the enactment of the Surface Mine Control and Reclamation Act (SMCRA) of 1977, operators were not required to reclaim surface mine sites and restore the landscape to "approximate original contour" (Zipper et al., 1989, 2011; Yonk et al., 2019; and Zipper and Skousen, 2021). As a result, anthropogenic alterations of the physical landscape and its associated landforms have added further geomorphic complexity to this region. Un-reclaimed, pre-SMCRA surface coal mine sites in this region are characterized by nearly flat mine benches and adjacent highwalls, which correlate with the site of coal extraction. These features tend to be long and narrow and follow the original topographic contour of the landscape. Figure 1 provides examples of these features as represented in a hillshade image generated from a light detection and ranging (lidar)–derived digital terrain model (DTM) (Figure 1a) and high-spatial-resolution, leaf-off aerial orthophotography (Figure 1b). As demonstrated in this figure, these physical landscape alterations tend to be topographically distinct despite not always being evident in aerial imagery, especially following the re-establishment of vegetation.

This paper documents an initial exploration of slope stability downslope from pre-law, un-reclaimed mine sites, which we argue is an understudied issue despite having important land management, geotechnical, and reclamation implications. We relied on manual interpretation of lidar-derived terrain visualizations (e.g., hillshades) and aerial orthophotography. Manual interpretation was aided by surface mining extent polygons provided by the West Virginia Geological and Economic Survey (WVGES) Coal Bed Mapping Project (CBMP) (WVGES::Interactive Coal Bed Mapping Project, 2024) and historic mine extents extracted from U.S. Geological Survey (USGS) historic topographic maps (USGS, 2023). We specifically investigated potential differences in slope stability downslope from mine benches associated with different coal seams and potential associations with topographic slope and aspect. Although the geographic focus of this study was northern West Virginia, these pre-law landscape alterations are also prevalent in southwestern Virginia, southeastern Ohio, southern West Virginia, eastern Kentucky, and southwestern Virginia (Zipper et al., 1989; Zipper and Skousen, 2021), highlighting the value in researching and documenting this issue.

Figure 2 shows an example elevation profile across a mine bench feature, which highlights the drastic change in the local topography caused by mining. Figure 3 provides an example of a mine bench in Taylor County, WV, with notable slope instability. Downslope creep is associated with overburden material that was excavated to extract the coal measures and placed below the bench during the mining process (examples are marked with arrows). Both highwalls and benches are typically rock cuts, while waste rock and sediment displaced during the mine process were placed on the slopes beneath these features. Highwalls represent the site of coal removal, while mine benches are the remnant surfaces where the mine operation was undertaken. Although instabilities are prominent around this particular site, this is not the case for all sites mapped within the region. A visual comparison of slope stability around mine sites in which different coal seams were extracted suggests that failures may be more prominent downslope from surface mines within certain coal seams as opposed to others. Motivated by this observation, our working hypothesis was that mine-adjacent hillslope failure potential might vary according to the coal seam that was mined.

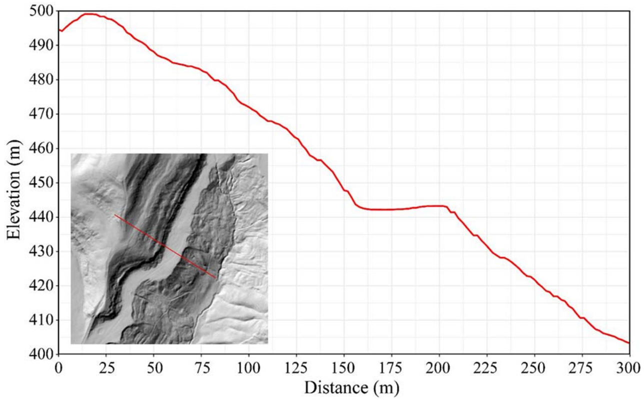

Figure 2. Example elevation profile for a mine bench location, which highlights the terrain alterations resulting from historic resource extraction practices.

BACKGROUND

Most work on post-mining geohazards in Appalachia has focused on areas that experienced mountaintop removal/valley fill (MTRVF) coal mining, a practice that became widespread after 1970, in which entire mountaintops are excavated using explosives, and displaced overburden material is deposited in adjacent valleys (Palmer et al., 2010; Bernhardt and Palmer, 2011; and Ross et al., 2016). The large-scale topographic alterations and environmental impacts associated with MTRVF mining have overshadowed the important landscape impacts of historic mining that occurred before the passage of the SMCRA. A review of the existing literature found no studies exploring topographic, landform, or geomorphic change associated with pre-law contour, highwall, and/or surface mining in Appalachia. Studies relating to historic mining in this region tend to focus on water-quality issues, such as acid mine drainage (e.g., Gray, 1997; Skousen et al., 2000; Johnson and Hallberg, 2005; Akcil and Koldas, 2006; and Simate and Ndlovu, 2014); post-mine soils and associated characteristics and productivity (e.g., Haering et al., 2004; Feng et al., 2019); and forest biomass, productivity, and ecology (e.g., Rodrigue et al., 2002; Zipper et al., 2011; and Sena et al., 2021). There is a clear knowledge gap relating to the geomorphology of, and geohazards associated with, historic mine benches and highwalls, despite their abundance within the Appalachian region and globally. Even areas that have experienced more recent MTRVF mining have many un-reclaimed, pre-law mine benches and highwalls that have been overprinted with more recent mountaintop mining (Zipper and Skousen, 2021).

This study was made possible by the availability of lidar data over large spatial extents. Lidar has several benefits for creating DTMs representing bare earth surface conditions. When collected from an aerial platform, it is possible to create detailed representations of the bare earth surface (e.g., DTMs with a spatial resolution of less than 2 m). Data are also collected with high vertical and horizontal accuracies (e.g., less than 25 cm root mean square error). Since many systems allow for multiple returns to be recorded from a single laser pulse, it is

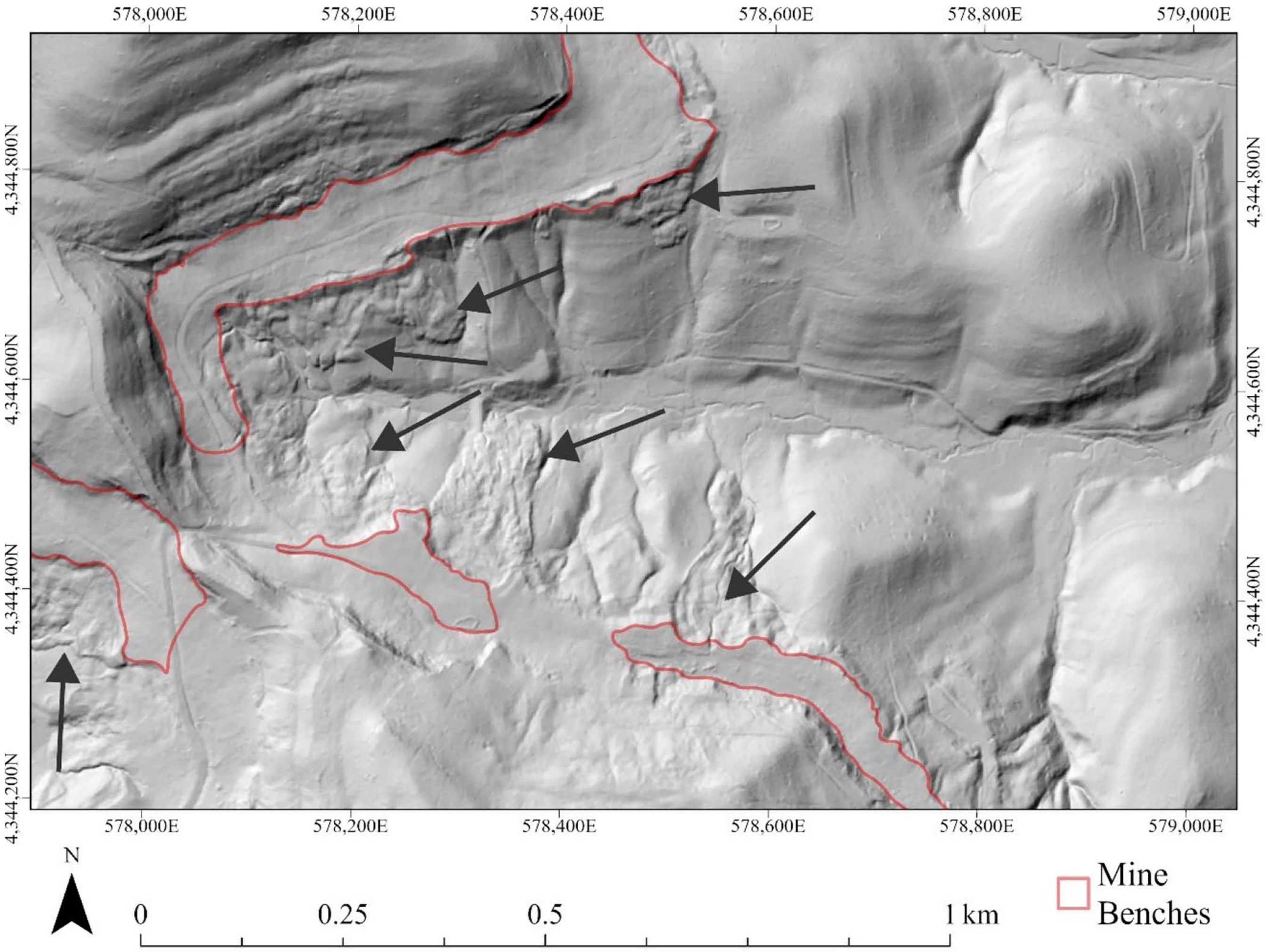

Figure 3. Example of a mine bench in Taylor County, WV, with notable slope failures or instability occurring downslope (examples are marked with arrows). The NAD83 UTM Zone 17N coordinate system is used.

possible to characterize the terrain surface even under a tree canopy, which is of importance in this study, since many of the historic surface mines in the Appalachian region are now at least partially reforested. Canopy penetration is generally not possible with other methods used to create DTMs or digital surface models, such as photogrammetry, radar, and drone-based structure-from-motion (Lillesand et al., 2015).

Due to the level of detail provided and the ability to characterize bare earth surfaces even under vegetation cover, lidar allows detailed mapping of landforms and geomorphic features (e.g., Jones et al., 2007; Notebaert et al., 2009; Johnson et al., 2015; and Singh et al., 2020). This is also true for archaeological mapping and research (e.g., Fernandez-Diaz et al., 2014; Hare et al., 2014; and Štular et al., 2021), which highlights the value of lidar for mapping both natural and anthropogenic landforms as well as physical landscape change. Lidar data have also been combined with machine learning and deep learning methods to identify and extract natural and anthropogenic landforms and features (e.g., Albrecht et al., 2019; Maxwell et al., 2020a; Fiorucci et al., 2022; and Maxwell et al., 2023). For example, Maxwell et al. (2020a) explored the use of lidar-derived terrain representations and deep learning–based instance segmentation for mapping mine-related valley-fill features in the MTRVF region, and Rafique et al. (2022) explored semantic segmentation deep learning for mapping sinkholes in the state of Kentucky. Unfortunately, the mine benches and slope failure/instability features of interest in this study have proven challenging to map using automated, deep learning–based methods. As a result, features were manually digitized for this study.

STUDY AREA

The study area lies in north-central West Virginia (Figure 4) and consists of 11 counties: Barbour, Grant,

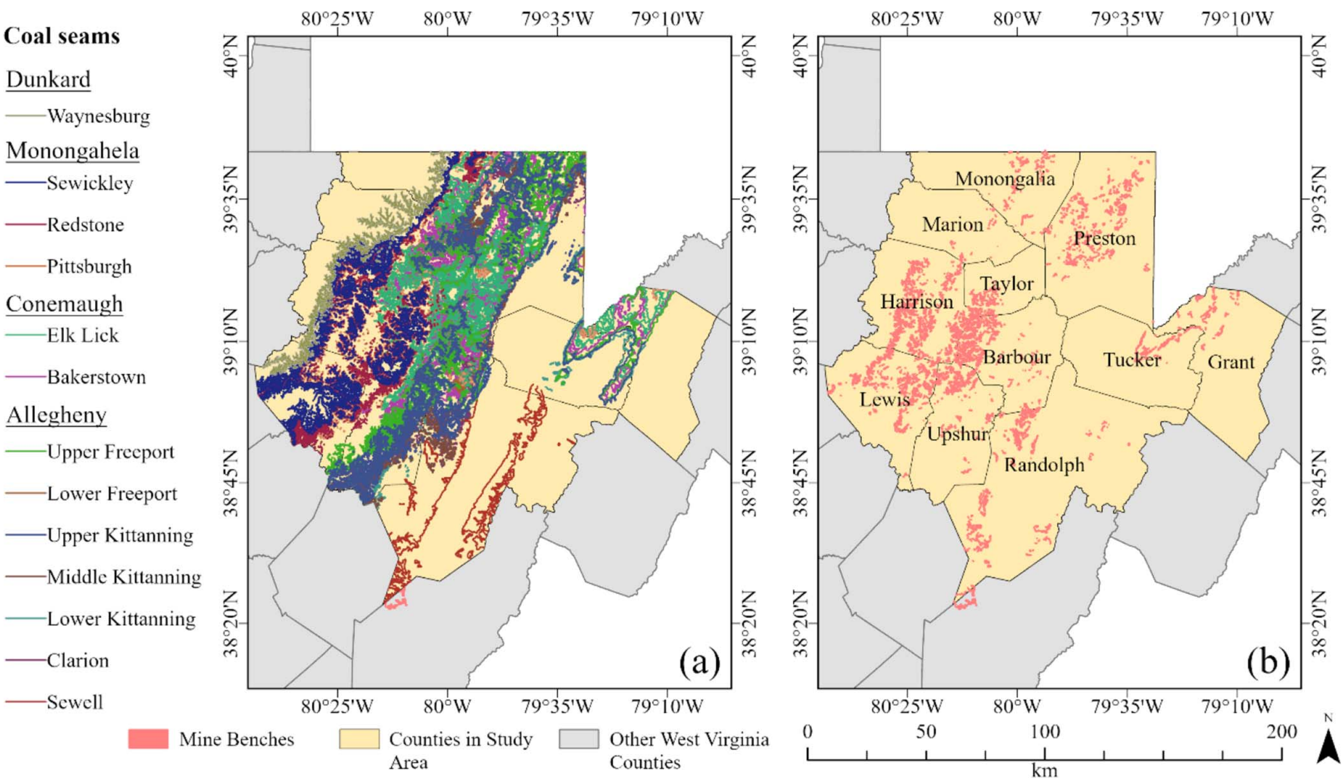

Figure 4. Location map of the study area in north-central West Virginia. (a) Coal seam outcrop data from the West Virginia Geological and Economic Survey (WVGES). (b) Red areas indicate mapped mine benches generated as part of this study.

Harrison, Lewis, Marion, Monongalia, Preston, Randolph, Taylor, Tucker, and Upshur. These counties were selected because they have experienced extensive pre-law surface coal mining, they host several different coal seams that have been mined (as discussed below), and they have not experienced more recent surface mining—such as the mountaintop mining found in the southern coalfields of West Virginia—that would overprint pre-law mining features and confound our analysis. Figure 4a shows coal-seam outcrop data provided by the WVGES, while Figure 4b shows the mine bench extents created as part of this study.

Our study area covered parts of the Appalachian Plateau and Allegheny Mountain Section physiographic provinces. Figure 5 shows the geologic periods and key structural features (fold hinges) occurring within the study area extent. Data presented here were derived from the 1:250,000-scale geologic map of West Virginia created by Cardwell et al. (1968). The coal seams occur within the Pennsylvanian Period stratigraphy, which dominates in the western extent of the study area. Folding causes the surface exposure of NE/SW-striking bands of Pennsylvanian strata in the eastern extent of the study area.

According to Freme and Hong (1999), there are three coal-producing regions in the Appalachian Basin: the northern region, which includes western Pennsylvania, eastern Ohio, western Maryland, and northern West Virginia; the central region, which includes southern West Virginia, eastern Kentucky, northern Tennessee, and southwestern Virginia; and the southern region, which includes southern Tennessee, Alabama, and Georgia. Our study area is situated within the northern

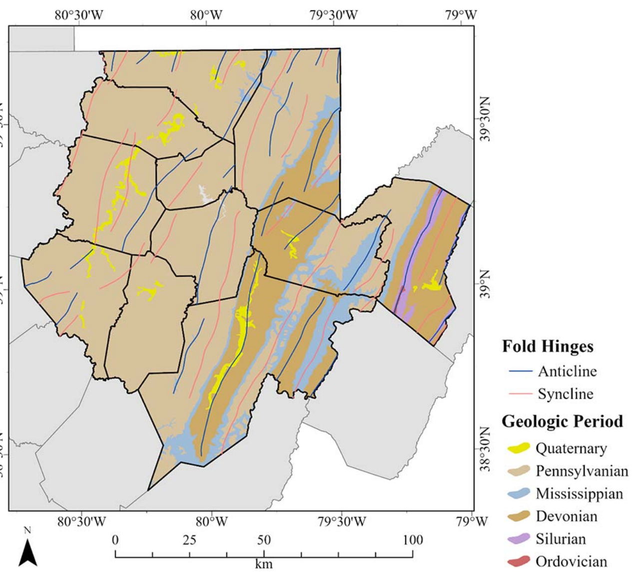

Figure 5. Geologic map of the study area showing geologic periods and fold hinges. Data are from the 1:250,000-scale geologic map of West Virginia created by Cardwell et al. (1968).

Table 1. *Coal seams and associated group or formation and geologic period. The count of mine benches and total area of mine benches per seam are based on the mapping undertaken for this study. Coal bed and overburden thickness data were aggregated from data provided by the West Virginia Geological and Economic Survey (WVGES)::Interactive Coal Bed Mapping Project (2024).*

Geologic Period	Group/Formation	Coal Seam	Bench Feature Count	Bench Area (km^2)	Coal Bed Thickness (Mean/Max) (m)	Overburden Thickness (Mean/Max) (m)
Permian/Pennsylvanian	Dunkard Group	Waynesburg	27	308	0.9/2.9	11.6/27.9
Pennsylvanian	Monongahela	Sewickley	45	1,299	1.0/3.5	13.7/35.6
		Redstone	414	4,224	0.7/2.4	14.2/35.6
		Pittsburgh	953	44,894	1.5/3.7	14.3/48.3
	Conemaugh	Elk Lick	47	1,414	0.5/1.8	11.0/38.1
		Bakerstown	161	15,966	0.6/2.4	11.5/43.2
	Allegheny	Upper Freeport	315	9,496	0.9/3.2	8.6/30.5
		Lower Freeport	39	688	0.5/2.3	9.6/40.6
		Upper Kittanning	20	297	0.6/3.2	10.8/35.6
		Middle Kittanning	178	3,789	0.8/4.3	10.6/40.6
		Lower Kittanning	35	589	0.7/3.8	9.6/43.2
		Clarion	2	15	0.7/2.7	12.9/38.1
		Sewell	112	2,577	0.7/4.3	16.3/71.2

region. From oldest to youngest, Pennsylvanian strata are differentiated into four groups: the Pottsville, Allegheny, Conemaugh, and Monongahela groups. The Dunkard Group overlies these four groups, is Permian to Pennsylvanian in age, and also contains coal seams (Freme and Hong, 1999).

Table 1 summarizes the coal seams occurring within the study area extent and their associated group or formation, geologic period, mean and maximum thicknesses, and overburden mean and maximum thicknesses. Coal bed and overburden thicknesses were derived from data provided by the WVGES CBMP. It should be noted that coal bed and overburden thicknesses are variable across the study area extent; thus, the numbers provided are general and not meant to represent site-level characteristics. Table 1 also includes the number of mine benches occurring within the coal seam, as mapped as part of this study, and the cumulative land area of all mine benches per seam. The count of bench features per seam ranges from two to 953. The Monongahela Formation contains the largest number of mine benches, which are associated with three different coal seams. The largest number of mapped benches and the largest land area are associated with the Pittsburgh coal seam. Other important coal seams, based on bench count and land area, include the Redstone, Upper Freeport, Middle Kittanning, and Bakerstown coal seams.

METHODS

Overview

This study consisted of the following components, which are explained in detail in the remainder of this section:

1. manual digitization of mine bench features throughout the study area extent using digital terrain data, imagery, and ancillary geospatial data;
2. stratified random selection of a subset of digitized mine benches per coal seam for which to perform interpretation of slope failure occurrence;
3. differentiation of sections of the mine bench lower margin with and without associated downslope instability;
4. creation of topographic variables from a lidar-derived DTM;
5. data summarization and aggregation; and
6. statistical analysis to compare the abundance of slope failures by coal seam and assess the correlation with topographic characteristics.

Input Data

Figure 6 provides examples of the input data used in this study to digitize the mine bench features. Digital terrain data were the primary data source in this study. Specifically, we generated and used a hillshade model with 1 m spatial resolution (Figure 6a), derived from a lidar-based DTM provided by the West Virginia GIS Technical Center (WVGISTC). We also created a multi-band terrain representation consisting of a topographic position index (TPI) (Maxwell and Shobe, 2022) generated using a 50 m circular radius window and the square root of topographic slope, and a more local TPI using an annulus window with a 2 m inner radius and 5 m outer radius (Figure 6c). These complementary terrain visualizations allowed for identification of mine benches and slope failure features. Additional geospatial data were used to inform the digitization of mine bench extents and slope failures and were especially useful for differentiating mine benches or failures from other features on

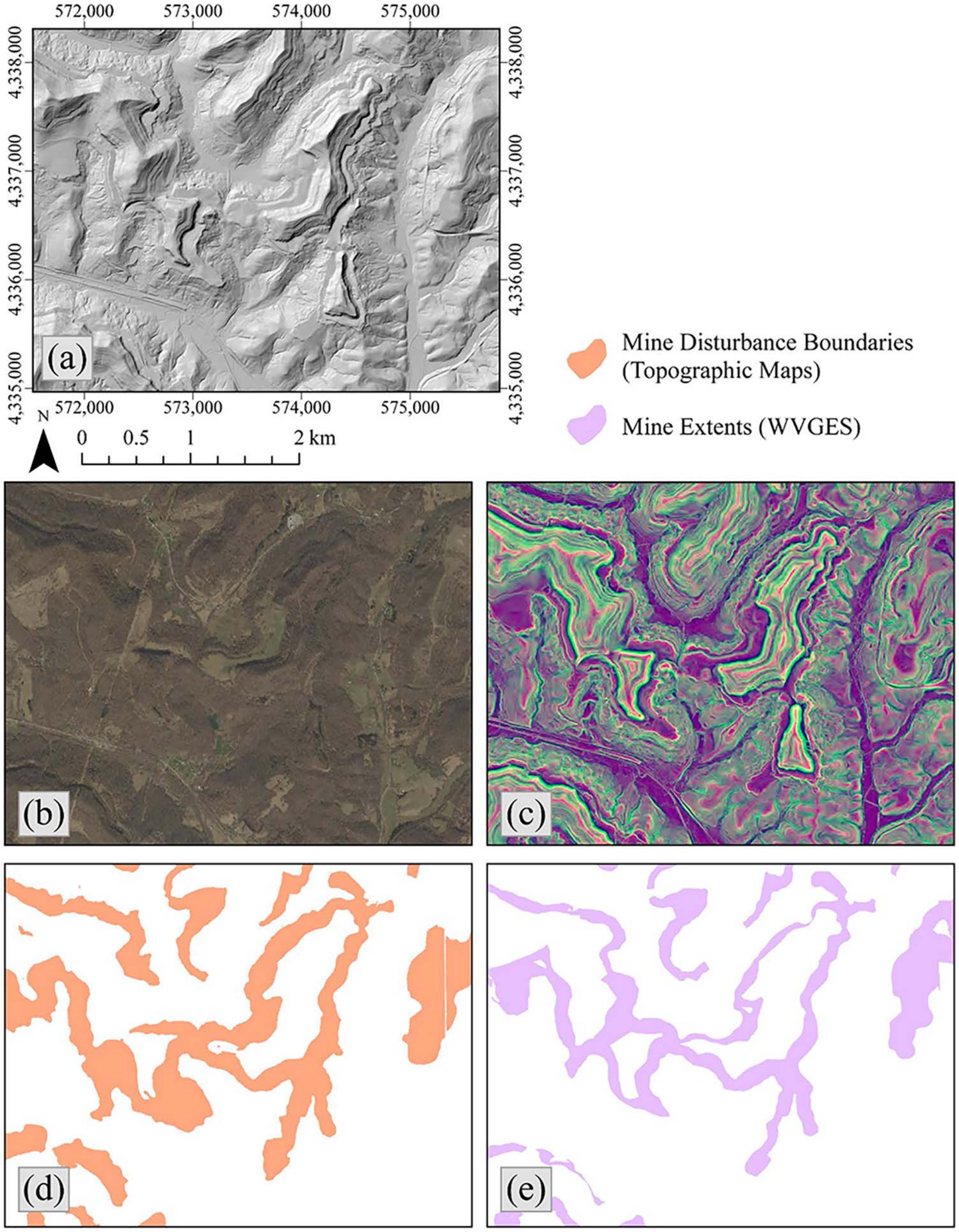

Figure 6. Example input data used to digitize mine bench extents: (a) 1-m-spatial-resolution hillshade model generated from lidar-derived DTM; (b) leaf-off aerial orthophotography from the West Virginia GIS Technical Center (WVGISTC); (c) multi-band terrain representation; (d) mine disturbance extents from historic U.S. Geological Survey (USGS) topographic maps; and (e) surface mine extents from the West Virginia Geological and Economic Survey (WVGES).

the landscape that can have a similar presentation, such as construction or road cuts. In this study, high-spatial-resolution, leaf-off, aerial orthophotography was used (Figure 6b), which was also provided as a raster tile service by the WVGISTC. To further aid in digitization and to minimize false positive errors, we used historic surface mine boundaries, which were manually digitized from historical topographic maps provided by the USGS (USGS, 2023) (Figure 6d) and surface mine extents from the WVGES CBMP (WVGES::Interactive Coal Bed Mapping Project, 2024) (Figure 6e). To aid in the identification of slope failures, we used a statewide data set of slope failure initiation locations, which was provided by the WVGISTC. This data set was created by manual interpretation of the lidar-derived hillshade data and other ancillary data sources.

Digitization and Data Preparation

Features were digitized into a feature layer hosted on ArcGIS Online, which allows for multiple users to view and edit the data concurrently. All digitization was

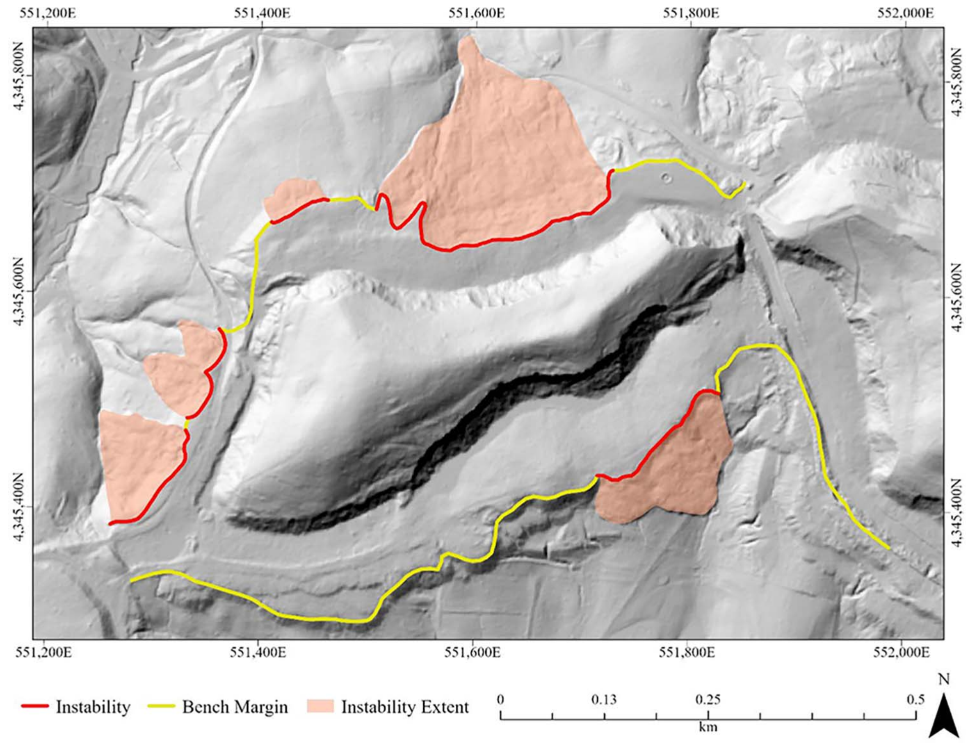

Figure 7. Example of second stage of digitization and manual interpretation required for this study. Red lines represent sections of the lower perimeter of the mine bench with associated slope failures, while yellow sections do not have associated slope failures. The red extents represent slope failures; however, the full extent of slope failures is not easy to consistently interpret for all failure/instability extents. The NAD83 UTM Zone 17N coordinate system is used.

conducted at scales larger than 1:4,000 with the goal of capturing the full extent of mine benches and to produce a complete mapping of these features for the study area extent. These mine benches were digitized, as opposed to using the existing USGS or WVGES CBMP data referenced above, because it was necessary to refine the boundaries to align with the topographic presentation of the mine benches as characterized on the lidar-derived hillshades for use in this study. Although the existing data sets were of high quality, they did not always align well with the topographic presentation of landscape change observed in the hillshade visualizations. Thus, we found it necessary to develop a new data set using the topographic presentation of the mine benches within the high-spatial-resolution terrain data as the primary source.

Additional data were required for this study. Specifically, we (1) associated each mine bench with the coal seam from which it was mined, (2) extracted the length of the lower (downslope) perimeter of each mine bench, and (3) identified sections of the lower perimeter that exhibited associated slope failures or instability in the downslope direction. To identify the coal seam associated with each mine bench, we performed spatial joins to extract the attribute information from the WVGES CBMP data, associating it with the spatially co-occurring mine benches in our digitized data set.

To quantify slope failure density downslope from historic mine benches, 30 digitized mine extents per coal seam were randomly selected, with a focus on seams having at least 100 mapped benches. Based on the summary presented in Table 1, the following seams were included in the analysis: Redstone, Pittsburgh, Bakerstown, Upper Freeport, Middle Kittanning, and Sewell. Figure 7 provides a conceptualization of the second stage of digitization. For each of the randomly selected mine benches, stratified by coal seam, we extracted the lower perimeter as a vector line feature from the previous digitized data set. Next, we partitioned the perimeter length into two categories for each mine bench: the length associated with instability and the length without notable instability. This allowed the calculation of the proportion or percentage of the lower perimeter length associated with failure/instability, which served as the estimate of or proxy for failure density. In Figure 7, we included the extent of slope failures around the margin of the mine; however, we did not map slope failure extent for all randomly selected mine benches because it was often difficult to map the areal extent of all failure or instability features. Instead, the proportion of the lower perimeter length impacted was used, since it could be more consistently and accurately delineated. A total of 268 km of lower perimeter length was manually interpreted. Lengths per seam ranged from 30.6 km (Bakerstone) to 61.2 km (Redstone).

Topographic Aspect and Slope

Although our primary objective was to explore the abundance of slope failures or instability beneath pre-law mine benches and any differences in abundance among coal seams, it is also important to consider additional confounding factors. Specifically, the abundance and occurrence of instability may be correlated with local topographic slope, which is not consistent across the study area (Maxwell et al., 2020b; Maxwell et al., 2021a, 2021b). Local slope changes across the study area due to spatial heterogeneity in bedrock dip angle, thickness and erodibility of strata, and incision depth of the stream network. The topographic aspect, or compass direction the slope is facing, may also be a factor influencing slope failure potential, since aspect can impact daily temperature fluctuations, incoming solar insolation, and moisture levels (Franklin, 2020; Maxwell and Shobe, 2022).

To explore the impacts of topographic slope and aspect, we first calculated these surfaces as raster grids with 1 m spatial resolution from the lidar-derived DTM using the Slope and Aspect tools in ArcGIS Pro (ESRI, 2024), respectively. Due to the circular nature of aspect when represented as a compass direction, it was converted into two separate measures: The sine of aspect was calculated as a measure of "eastwardness," while the cosine of aspect was calculated as a measure of "northwardness." Using aspect in radians, the eastwardness transformation resulted in east-facing slopes being represented by a value of 1 and west-facing slopes being represented by a value of -1. For northwardness, north-facing slopes are represented by a value of 1, and south-facing slopes are represented by a value of -1 (Stage, 1976). The aspect data were extracted at point locations spaced 5 m apart along the lower extents of each mine bench. This spacing was used to avoid double-sampling cells from the DTM data and its derivatives. Combining these aspect measurements with the classification of line segments as associated or not associated with failure/instability allowed for the comparison of aspect conditions between these two categories and differentiated by coal seams.

For topographic slope, we were primarily interested in considering pre-mining slope conditions. As a result, we first digitized at least five transects for each sampled mine bench that were perpendicular to the mine bench and upslope from it. We chose to use upslope positions, hypothesizing that these surfaces were more representative of the pre-mining landscape. Slopes downslope of mine benches are commonly modified by the mining operation and the placement of overburden or displaced material over the original slopes, potentially resulting in a decrease in slope in comparison to pre-mining conditions. As with aspect, slope measurements along these transects were calculated at point locations placed 5 m apart. The average slope conditions were then associated with the mine bench based on spatial proximity.

Figure 8 shows examples of the digitized results, including segmentation of the lower mine bench margin into regions with interpreted failures/instability and regions without interpreted failures/instability as line features, which are differentiated using red and yellow colors, respectively. Example transects are shown in blue, and sample point locations along the transects and mine bench lower margins are shown as black dots within the inset map.

Statistical Comparison of Slope Failure Abundance

Exploratory data analysis suggested that these data violated the assumptions of the parametric analysis of variance (ANOVA) test for comparing differences between groups with the primary issue being non-homogeneity of variance. As a result, a non-parametric Kruskal-Wallis test was used followed by a non-parametric pairwise comparison (Kruskal and Wallis, 1952). The goal of this test is to assess for differences between groups using ranks and medians. Specifically, we tested for differences between coal seams with regard to the proportion of the lower margin length associated with slope failures or instability. Correlations between slope and topographic aspect with failure/instability occurrence were investigated using Spearman correlation coefficients (Dodge, 2008).

RESULTS

Slope Failure Abundance Differences Between Coal Seams

Table 2 and Figure 9 summarize our visual-based assessment of the percentage of the mine bench outer perimeter length associated with slope failures or instability for the randomly selected benches. Benches associated with the Pittsburgh and Redstone seams have a larger percentage of their lower margin length associated with failures in comparison to the other seams investigated, as highlighted by the summarized distributions for these seams in the table and figure and, notably, the larger third-quartile values for the Pittsburgh and Redstone seams and the larger mean and median for the Pittsburgh seam. Failures were generally not abundant beneath the other investigated seams, except for a small subset of the randomly selected benches. Note that the point features in Figure 9 represent outliers, which are defined as samples that have

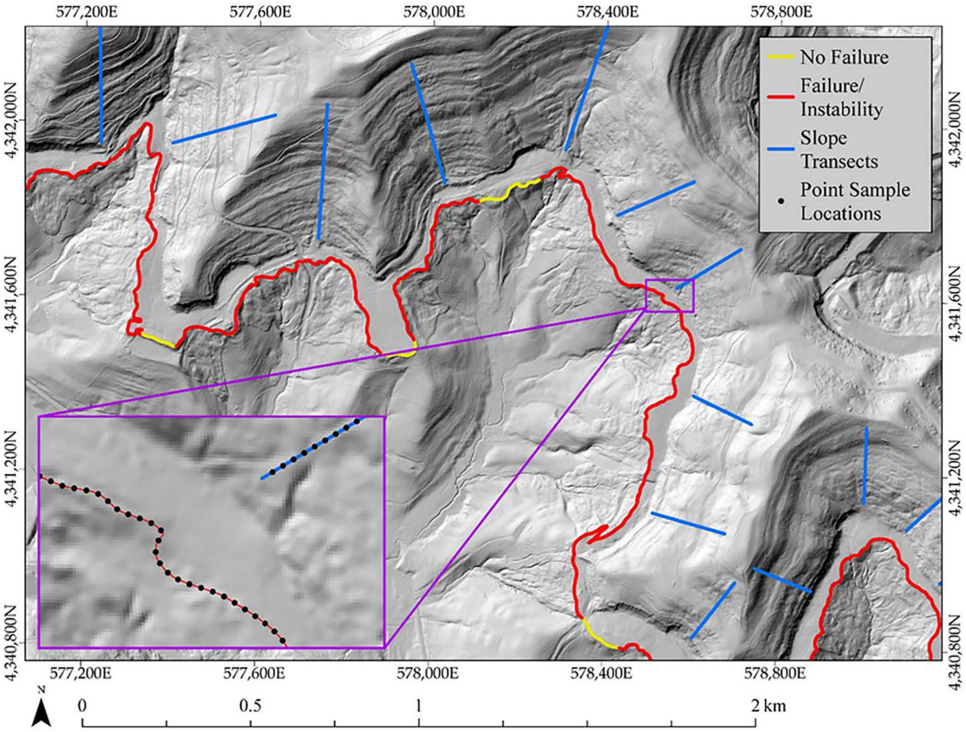

Figure 8. Digitized results with lower mine bench margins segmented into failure/instability (red) and no failure/instability (blue) regions. Yellow lines show example transects; black dots indicate sample point locations. The NAD83 UTM Zone 17N coordinate system is used.

high values farther than 1.5 inter-quartile range (IQR) from the third quartile. Outliers with low values are defined as those with values further than 1.5 IQR from the first quartile. This same definition of outliers is used in the remaining graphs presented here. No low outlier values were documented because the central tendency of most distributions of failure percentage is near zero.

The Kruskal-Wallis test suggested that at least two seams showed statistically significant differences (Kruskal-Wallis chi-squared = 29.25, degrees of freedom = 5, p value = 2.1e−5) in percent of lower margin lengths associated with failure/instability, as estimated using ranks and medians. As a result, subsequent pairwise comparison was merited. Table 3 presents the results of this pairwise comparison. A 95 percent confidence interval (CI), or a multiple-hypothesis-adjusted p value lower than 0.05, was used to define a statistically significant difference between pairs. Also, if a value of zero occurs between the lower and upper 95 percent CI bounds, then the pair of seams does not have a statistically significant difference in percent of their lower margin associated with failures/instability.

Using a 95 percent CI, a statistical difference was suggested between the Pittsburgh seam and all other investigated seams other than the Redstone seam (p value = 9.13e−1). No other coal seams were suggested to be statistically different. Notably, the Redstone seam, which also had some randomly selected benches with larger percentages of their lower margins associated with failures/instability, was not suggested to be statistically different from any other investigated seam. In short, slope

Table 2. *Summary statistics associated with frequency of slope instability around mine benches with results differentiated by coal seam.*

Coal Seam	Number of Mine Benches Sampled	Mean Total Length (m)	Median Total Length (m)	Mean Length of Instability (m)	Median Length of Instability (m)	Mean Percent of Length with Instability	Median Percent of Length with Instability
Redstone	30	2,039.0	1,112.8	735.9	0.0	13.3%	0.0%
Pittsburgh	29	1,467.8	1,087.3	602.1	185.4	17.7%	7.1%
Bakerstown	29	1,034.1	798.5	116.6	0.0	3.7%	0.0%
Upper Freeport	30	1,028.8	784.5	31.4	0.0	3.2%	0.0%
Middle Kittanning	29	1,540.9	893.0	26.1	0.0	1.5%	0.0%
Sewell	30	1,888.4	1,382.0	10.3	0.0	1.7%	0.0%

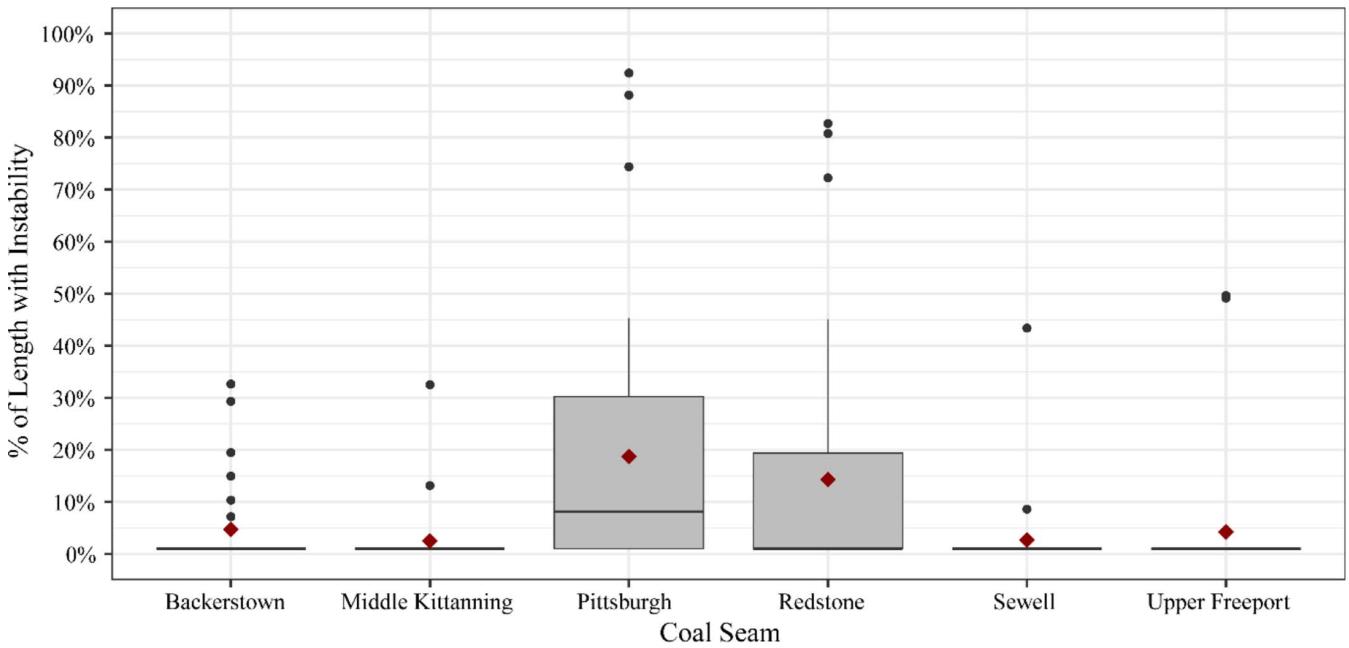

Figure 9. Box plot summarizing the distribution of percentage of the lower perimeter length associated with slope failures or instability for each investigated coal seam using randomly selected benches. The interquartile range (IQR) is shown in gray. The center black line in the interquartile range represents the median value. Red diamonds represent the mean value, while black points represent outliers. Outliers are defined as high values that are more than 1.5 IQR from the third quartile or low values that are more than 1.5 IQR from the first quartile.

failure abundance was suggested to be most clearly associated with the Pittsburgh seam.

Topographic Slope and Aspect

Table 4 provides the Spearman correlation coefficients between topographic slope and percent of lower margin length with slope failures/instability for different coal seams. The Pittsburgh seam has a moderately negative, but not statistically significant, correlation (−0.227, p value = 0.237), which is unexpected. The Bakerstown, Middle Kittanning, Sewell, and Upper Freeport seams show very weak correlations. The Redstone seam has a weakly positive, but not statistically significant, correlation (0.129, p value = 0.498). Overall, the correlation analysis suggests that uphill, pre-mining topographic slope is not strongly associated with failure or instability abundance. Generally, and in contrast to results suggesting that failures are

Table 3. *Kruskal-Wallis pairwise-comparison results between each pairwise combination of coal seams for percentage of the lower perimeter length associated with slope failures or instability calculated using randomly selected benches.*

Seams Compared	Difference	Lower 95% CI	Upper 95% CI	Adjusted p Value
Bakerstown vs. Middle Kittanning	10.97	−16.81	38.74	1.00
Bakerstown vs. Pittsburgh	−28.86	−56.64	−1.09	3.43e−2
Middle Kittanning vs. Pittsburgh	−39.83	−67.60	−12.05	3.85e−4
Bakerstown vs. Redstone	−11.27	−38.82	16.27	1.00
Middle Kittanning vs. Redstone	−22.24	−49.78	5.30	2.67e−1
Pittsburgh vs. Redstone	17.59	−9.95	45.13	9.13e−1
Bakerstown vs. Sewell	11.13	−16.42	38.67	1.00
Middle Kittanning vs. Sewell	0.16	−27.38	27.70	1.00
Pittsburgh vs. Sewell	39.99	12.45	67.53	3.04e−4
Redstone vs. Sewell	22.40	−4.91	49.71	2.41e−1
Bakerstown vs. Upper Freeport	10.13	−17.42	37.67	1.00
Middle Kittanning vs. Upper Freeport	−0.84	−28.38	26.70	1.00
Pittsburgh vs. Upper Freeport	38.99	11.45	66.53	4.88e−4
Redstone vs. Upper Freeport	21.40	−5.91	48.71	3.22e−1
Sewell vs. Upper Freeport	−1.00	−28.31	26.31	1.00

Table 4. *Spearman correlation coefficients and p values for percent of lower margin length with associated slope failures or instability compared to topographic slope by coal seam.*

Coal Seam	Spearman Correlation Coefficient	*p* Value
Bakerstown	−0.068	0.725
Middle Kittanning	−0.174	0.367
Pittsburgh	−0.227	0.237
Redstone	0.129	0.498
Sewell	−0.034	0.859
Upper Freeport	0.072	0.705

associated with particular coal seams, this initial study did not document a strong correlation between topographic slope and failure abundance.

Similar to topographic slope, sections of the lower margin impacted by failure/instability were not strongly associated with particular ranges of slope orientations or aspects, as measured with eastwardness (Figure 10) and northwardness (Figure 11). Distributions of eastwardness and northwardness showed similar medians and IQRs between benches associated with the same seam but with and without associated failures or instabilities. For northwardness, some differences were noted for the Middle Kittanning and Upper Freeport seams. However, these seams generally had a lower abundance of failures, so these results could be explained by the small sample size in the lengths associated with failures. In summary, similar to topographic slope, we did not document a strong correlation between aspect and slope failure abundance in this initial study.

DISCUSSION

Summary of Findings

There is generally a lack of research on the long-term slope stability of mining-impacted regions and hillslopes, especially pertaining to pre-law, un-reclaimed mine bench features. Prior work by Reed and Kite (2020), using a combination of fieldwork and interpretation of lidar-derived terrain surfaces, documented gully formation and associated erosion on or near valley-fill faces associated with mountaintop removal coal mine reclamation. Similarly, our study suggests that pre-law mine benches, though typically smaller in size than mountaintop removal mines, may also face issues of long-term slope stability. Despite their smaller size in comparison to mountaintop mine operations, they are abundant in the region and may be an important management concern.

The extent of mining-associated hillslope failures varies by coal seam. The Pittsburgh seam, with a mean of 17.7 percent of the lower margin lengths associated with failures/instabilities for randomly selected mine benches, and the Redstone seam, with 13.3 percent, showed higher rates of slope failure occurrence than the other investigated seams. The pairwise Kruskal-Wallis tests suggested significant differences between the Pittsburgh seam and all other seams other than the Redstone seam. The Redstone seam did not show statistical difference between any of the other seams. This initial analysis also suggests that there is not a strong correlation between local topographic slope or topographic aspect and slope failure/instability occurrence. In summary, slope and aspect do not appear to be drivers of slope failure occurrence beneath historic, pre-law mine benches in the investigated region; however, failure/instability is more prominent beneath mine benches associated with the Pittsburgh and Redstone seams. It should be noted that these two seams are stratigraphically close; as a result, some mine sites may have been excavating both seams. In other words, the seam associated with the bench, as provided by the WVGES, may have had some errors or uncertainties. Both the Pittsburgh and Redstone

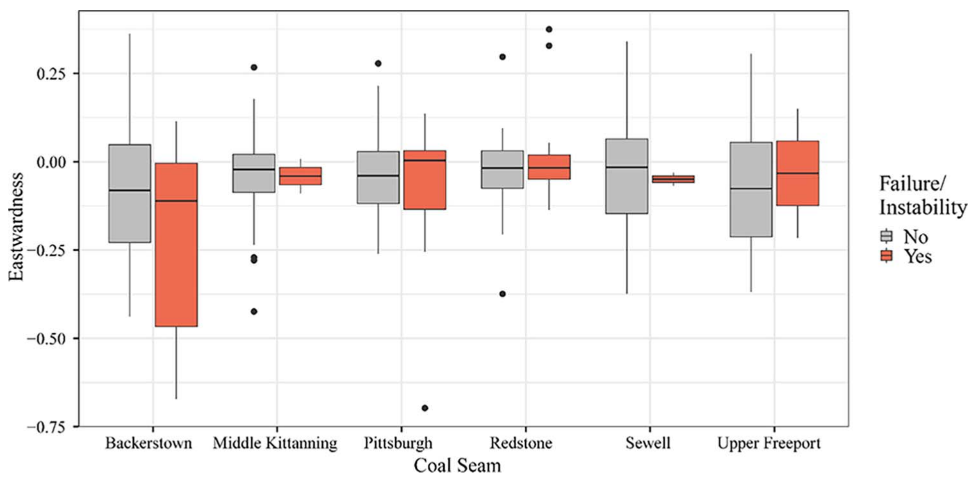

Figure 10. Box plots comparing eastwardness values between sections of the lower margin with and without associated failure/instability for each investigated coal seam.

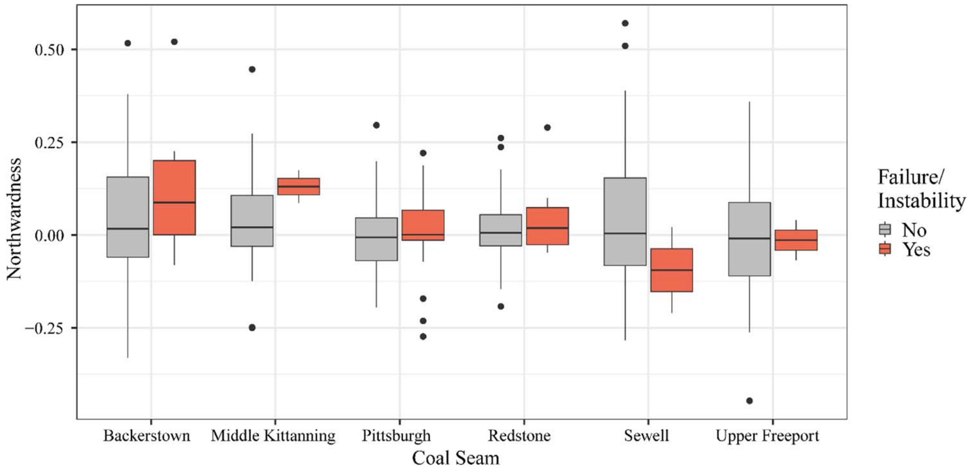

Figure 11. Box plot comparing northwardness values between sections of the lower margin with and without associated failure/instability for each investigated coal seam.

seams occur within the Monongahela Group (Lyons, 1998).

Based on our interpretation of the lidar-derived terrain data and conversations with professional geologists at the WVGES and West Virginia Department of Environmental Protection (WVDEP), the material associated with downslope creep, instability, or failure is most likely material that was displaced by the mining process and deposited beneath the mine bench, rather than the original material constituting the pre-mining slope. Given that the units/formations of the Monongahela Group (Ruppert and Rice, 2000), other than coal, generally consist of shales or mudstone, which are generally erodible units, it is not surprising that displaced overburden material derived from these units may be prone to instability. In contrast, coal seams occurring in the Allegheny Formation are often surrounded by sandstone units that may be less prone to erosion or instability (Ruppert and Rice, 2000). Another potential contributing factor is the thickness of the coal seams. The Pittsburgh seam, on average, is generally thicker than the other seams included in the study (see thickness data from the WVGES provided in Table 1) (Ruppert and Rice, 2000). Although thicknesses vary, the Pittsburgh seam averages ~1.5 m in thickness, with some additional thickness added by the Pittsburgh rider coal bed, which occurs above the larger seam and is often mined alongside it. The Redstone seam can be up to ~2.4 m thick (Roen et al., 1968). The thickness of the overburden may also play a role. For example, the Pittsburgh seam has a mean overburden thickness of 14.3 m and a maximum thickness of 48.3 m. The Pittsburgh and Redstone seams had the highest mean overburden thicknesses, 14.3 m and 14.2 m, respectively, of all the seams included in the study other than the Sewell seam of the Allegheny Group (mean = 16.3 m). This could also contribute to failure abundance and the amount of displaced material. The available data do not allow us to assess either site-specific amounts of displaced overburden or the characteristics of these materials.

Limitations and Future Research

Our interpretations are limited by a lack of *in situ* geotechnical data with which to characterize the mine benches and their adjacent hillslope failures as well as a lack of multi-temporal remote-sensing information with which to establish the timing of hillslope failures. Figures 12 and 13 illustrate the complexity associated with pre-law mining sites and associated hillslope failures. The mine bench is obvious in the lidar-derived hillshade image (Figure 12a). However, it is less obvious in the leaf-off aerial imagery (Figure 12b), other than the lack of woody vegetation on sections of the bench surface. As evident in the hillshade image, downhill creep is noted beneath the bench, suggesting issues of slope instability. Figure 13 shows a series of photos taken at the site and within the extent of the blue box in Figure 12a and b. The first two images (Figure 13a and b) were taken directly beneath the highwall and on the mine bench. The images in Figure 13c and d were taken beneath the mine bench and within the region of lidar-interpreted slope instability. These images highlight the complexity of characterizing hillslope conditions around mine benches, even with site visits, due to vegetation cover. The downhill creep so readily evident in the hillshade image is not easily observable in the field.

The establishment of vegetation may stabilize downhill creep features, and the creep may be a remnant of the time period during or directly following the mining operations and prior to the establishment of vegetation. Given the lack of historic, multi-temporal, high-spatial-resolution digital terrain data, it is not possible to

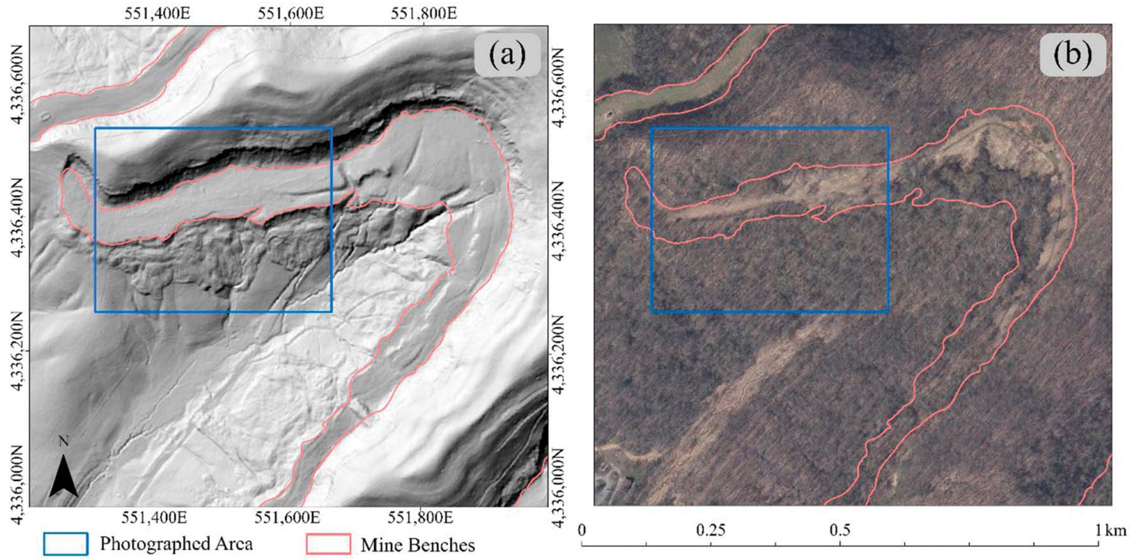

Figure 12. Mine bench within Watters Smith Memorial Park shown in the lidar-derived hillshade model (a) and leaf-off aerial imagery (b). The photographs shown in Figure 13 were taken within the extent outlined in blue. The NAD83 UTM Zone 17N coordinate system is used.

analyze change over time, since detailed terrain textures are not captured in historic, photogrammetrically derived digital elevation models. A full temporal understanding of slope instability and downhill creep within this region merits field-based, site-specific assessment to characterize the stability of the unconsolidated overburden materials placed on the slopes beneath the bench as well as analysis of multi-temporal remote-sensing data sets. It would also be of value to interview property owners and residents who have observed terrain changes and revegetation processes over decades.

To investigate how mine benches may impact landscape evolution processes, it would be interesting to make use of numeric modeling methods such as those used by Bower et al. (2024) in the mountaintop mining region. It is an open question whether there exist sufficient data on the erodibility of both undisturbed and disturbed earth materials to extract actionable predictions from these models. Lack of characterization of the displaced unconsolidated materials beneath the mine benches may especially hinder such analyses, and fieldwork would likely be necessary to parameterize models and further characterize sites.

Applications to Land Management

This study has practical implications for land management and mine reclamation in the northern coalfields of Appalachia, and in other steep landscapes that have experienced similar styles of mining. The large numbers of pre-law, un-reclaimed mine benches in our study region may pose challenges in the future for property owners, communities, utility providers, and regulators, especially if future field-based research suggests that naturally established vegetation is not sufficiently stabilizing mining-impacted slopes. Locally, our work suggests that field validation and assessment might be best focused on benches associated with the Pittsburgh seam. More broadly, our results suggest that coal seam thickness and overburden lithology may be important controls on post-mining hillslope failure. If funds are made available to reclaim pre-law mine sites, we suggest that slope instability issues may be an important consideration in prioritizing projects. Our findings suggest that more work is needed to understand appropriate geotechnical and reclamation practices for long-term management of pre-law mine sites.

CONCLUSIONS

This study documented evidence of substantial slope instability beneath pre-law, un-reclaimed mine benches within a subsection of the northern coalfields of Appalachia. Topographic slope and aspect did not correlate with the occurrence of instability in this initial study. Instead, the coal seam associated with the bench was found to be the dominant factor, with instability being more abundant beneath benches associated with the Pittsburgh and, to a lesser degree, Redstone seams of the Monongahela Group. We hypothesize that this may be attributed to the historic mining practice of placing displaced overburden rock on the slopes beneath the bench, as well as to the characteristics of this overburden material, which was derived from relatively weak rock units overlying the coal seams. The thickness of the coal seam

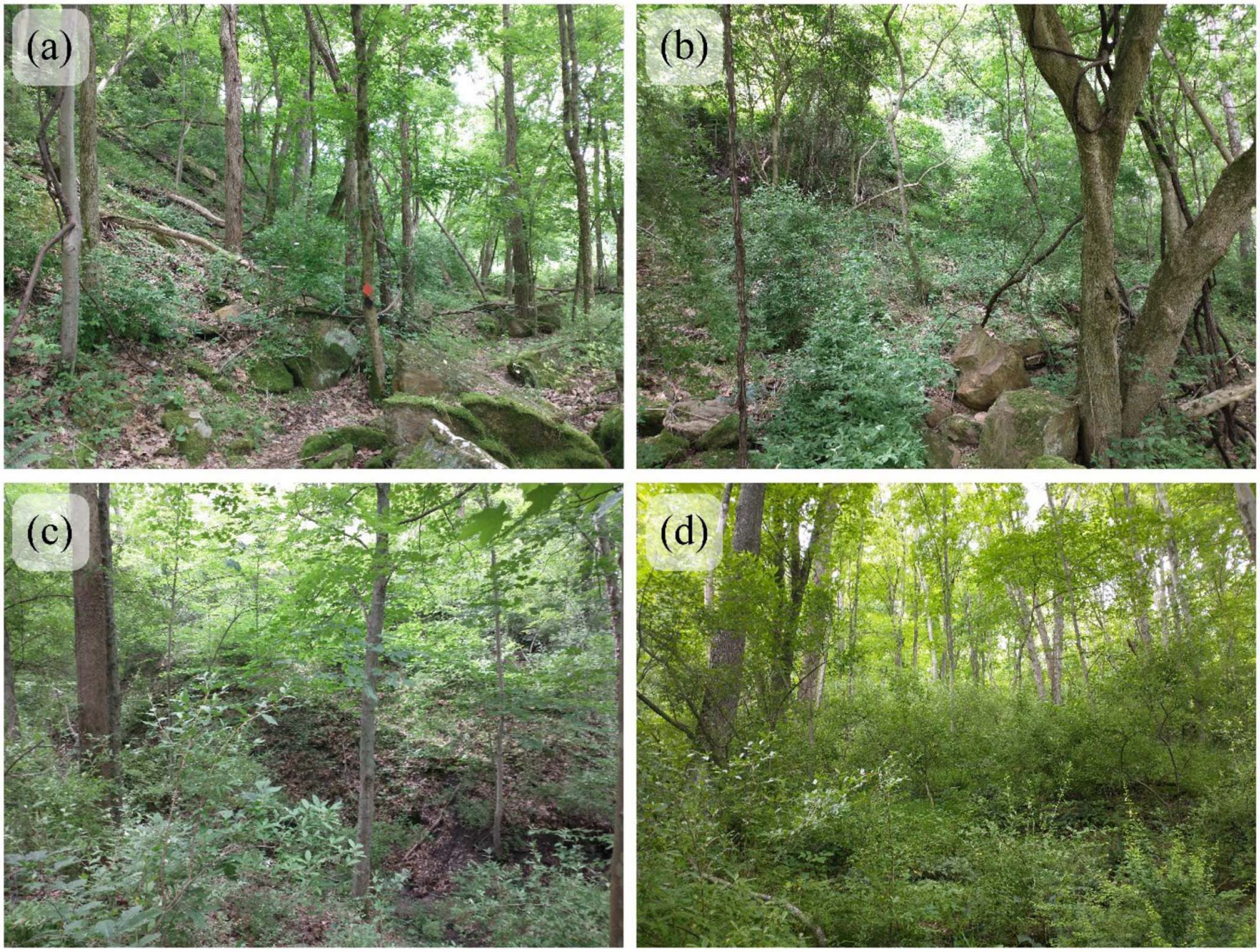

Figure 13. Example pre-law mine bench located in Watters Smith Memorial Park in Harrison County, WV. (a, b) Images taken directly below the highwall and on the mine bench within the area highlighted in Figure 12 using the blue box. (c, d) Images showing forested areas downslope from the mine bench, also occurring within the extent highlighted with the blue box in Figure 12, where slope instability was noted based on interpretation of the hillshade data.

extracted may also be a factor. Results suggest that local geology may play an important role in determining the response of steep landscapes to mining and other human disturbances.

This study documents the need for additional site-specific and field-based assessment to inform whether vegetation is able to effectively stabilize slopes in mined areas and, if instability is of concern, to determine the methods that can be used to provide long-term management of these relics of historic surface mining.

ACKNOWLEDGMENTS

The authors would like to thank two anonymous reviewers whose comments strengthened the work. We would also like to thank the West Virginia Geological and Economic Survey (WVGES) and the West Virginia GIS Technical Center (WVGISTC) for providing data used in the study. Thanks go to Dr. Jamie Toro for his guidance during the project. Funding for this research was provided by the National Science Foundation (NSF) (federal award ID no. 2046059: “CAREER: Mapping Anthropocene Geomorphology with Deep Learning, Big Data Spatial Analytics, and LiDAR”). Any opinions, findings, and conclusions or recommendations expressed in this material are those of the authors and do not necessarily reflect the views of the National Science Foundation. The findings and conclusions in this publication are those of the authors and should not be construed to represent any official U.S. Department of Agriculture or U.S. government determination or policy.

Author Contributions

Ali is the lead author of this study. He generated the mine bench data used in the study; conducted experiments, data summarization, and formal analysis; and drafted the original manuscript. Maxwell supervised and obtained funding for the study. Both Maxwell and Shobe assisted with study design, data interpretation, and editing the original draft. Farhadpour and Maxwell worked with Ali to generate the mine bench data and assisted in data analysis.

REFERENCES

Akcil, A. and Koldas, S., 2006, Acid mine drainage (AMD): Causes, treatment and case studies: *Journal of Cleaner Production*, Vol. 14, No. 12–13, pp. 1139–1145.

Albrecht, C. M.; Fisher, C.; Freitag, M.; Hamann, H. F.; Pankanti, S.; Pezzutti, F.; and Rossi, F., 2019, Learning and recognizing archeological features from LiDAR data. In *Proceedings of the 2019 IEEE International Conference on Big Data (Big Data)*: IEEE, Piscataway, NJ, pp. 5630–5636.

Bernhardt, E. S. and Palmer, M. A., 2011, The environmental costs of mountaintop mining valley fill operations for aquatic ecosystems of the Central Appalachians: *Annals of the New York Academy of Sciences*, Vol. 1223, No. 1, pp. 39–57.

Bower, S. J.; Shobe, C. M.; Maxwell, A. E.; and Campforts, B., 2024, The uncertain future of mountaintop-removal-mined landscapes 2: Modeling the influence of topography and vegetation: *Geomorphology*, Vol. 446, p. 108985.

Cardwell, D. H.; Erwin, R. B.; and Woodward, H. P., 1968, *Geologic Map of West Virginia*: West Virginia Geological and Economic Survey, Morgantown, WV.

Coates, D. R., 1977, *Landslides*: Geological Society of America Reviews in Engineering Geology III.

Dodge, Y., 2008, Spearman rank correlation coefficient. In *The Concise Encyclopedia of Statistics*: Springer, New York, NY, pp. 502–505.

ESRI, 2024. *Desktop GIS Software | Mapping Analytics | ArcGIS Pro*: Electronic software, available at https://www.esri.com/en-us/arcgis/products/arcgis-pro/overview

Feng, Y.; Wang, J.; Bai, Z.; and Reading, L., 2019, Effects of surface coal mining and land reclamation on soil properties: A review: *Earth-Science Reviews*, Vol. 191, pp. 12–25.

Fernandez-Diaz, J. C.; Carter, W. E.; Shrestha, R. L.; and Glennie, C. L., 2014, Now you see it. . . now you don't: Understanding airborne mapping LiDAR collection and data product generation for archaeological research in Mesoamerica: *Remote Sensing*, Vol. 6, No. 10, pp. 9951–10001.

Fiorucci, M.; Verschoof-Van Der Vaart, W. B.; Soleni, P.; Le Saux, B.; and Traviglia, A., 2022, Deep learning for archaeological object detection on LiDAR: New evaluation measures and insights: *Remote Sensing*, Vol. 14, No. 7, p. 1694.

Franklin, S. E., 2020, Interpretation and use of geomorphometry in remote sensing: A guide and review of integrated applications: *International Journal of Remote Sensing*, Vol. 41, No. 19, pp. 7700–7733.

Freme, F. L. and Hong, B., 1999, US coal supply and demand: 1999 review: *Electric Power*, Vol. 896, No. 922, pp. 937–938.

Froude, M. J. and Petley, D. N., 2018, Global fatal landslide occurrence from 2004 to 2016: *Natural Hazards and Earth System Sciences*, Vol. 18, No. 8, pp. 2161–2181.

Gray, N., 1997, Environmental impact and remediation of acid mine drainage: A management problem: *Environmental Geology*, Vol. 30, pp. 62–71.

Haering, K. C.; Daniels, W. L.; and Galbraith, J. M., 2004, Appalachian mine soil morphology and properties: Effects of weathering and mining method: *Soil Science Society of America Journal*, Vol. 68, No. 4, pp. 1315–1325.

Hare, T.; Masson, M.; and Russell, B., 2014, High-density LiDAR mapping of the ancient city of Mayapán: *Remote Sensing*, Vol. 6, No. 9, pp. 9064–9085.

Hooke, R. L., 2000, On the history of humans as geomorphic agents: *Geology*, Vol. 28, No. 9, pp. 843–846.

Johnson, D. B. and Hallberg, K. B., 2005, Acid mine drainage remediation options: A review: *Science of the Total Environment*, Vol. 338, No. 1–2, pp. 3–14.

Johnson, M. D.; Fredin, O.; Ojala, A. E.; and Peterson, G., 2015, Unraveling Scandinavian geomorphology: The LiDAR revolution: *GFF*, Vol. 137, No. 4, pp. 245–251.

Jones, A. F.; Brewer, P. A.; Johnstone, E.; and Macklin, M. G., 2007, High-resolution interpretative geomorphological mapping of river valley environments using airborne LiDAR data: *Earth Surface Processes and Landforms*, Vol. 32, No. 10, pp. 1574–1592.

Kruskal, W. H. and Wallis, W. A., 1952, Use of ranks in one-criterion variance analysis: *Journal of the American Statistical Association*, Vol. 47, No. 260, pp. 583–621.

Lillesand, T.; Kiefer, R. W.; and Chipman, J., 2015, *Remote Sensing and Image Interpretation*: John Wiley & Sons, New York, NY.

Lyons, P. C., 1998, The central and northern Appalachian Basin—A frontier region for coalbed methane development: *International Journal of Coal Geology*, Vol. 38, No. 1–2, pp. 61–87.

Maxwell, A. E.; Odom, W. E.; Shobe, C. M.; Doctor, D. H.; Bester, M. S.; and Ore, T., 2023, Exploring the influence of input feature space on CNN-based geomorphic feature extraction from digital terrain data: *Earth and Space Science*, Vol. 10, No. 5, p. e2023EA002845.

Maxwell, A. E.; Pourmohammadi, P.; and Poyner, J. D., 2020a, Mapping the topographic features of mining-related valley fills using mask R-CNN deep learning and digital elevation data: *Remote Sensing*, Vol. 12, No. 3, p. 547.

Maxwell, A. E.; Sharma, M.; and Donaldson, K. A., 2021a, Explainable boosting machines for slope failure spatial predictive modeling: *Remote Sensing*, Vol. 13, No. 24, p. 4991.

Maxwell, A. E.; Sharma, M.; Kite, J. S.; Donaldson, K. A.; Maynard, S. M.; and Malay, C. M., 2021b, Assessing the generalization of machine learning–based slope failure prediction to new geographic extents: *ISPRS International Journal of Geo-Information*, Vol. 10, No. 5, p. 293.

Maxwell, A. E.; Sharma, M.; Kite, J. S.; Donaldson, K. A.; Thompson, J. A.; Bell, M. L.; and Maynard, S. M., 2020b, Slope failure prediction using random forest machine learning and LiDAR in an eroded folded mountain belt: *Remote Sensing*, Vol. 12, No. 3, p. 486.

Maxwell, A. E. and Shobe, C. M., 2022, Land-surface parameters for spatial predictive mapping and modeling: *Earth-Science Reviews*, Vol. 226, p. 103944.

Notebaert, B.; Verstraeten, G.; Govers, G.; and Poesen, J., 2009, Qualitative and quantitative applications of LiDAR imagery in fluvial geomorphology: *Earth Surface Processes and Landforms*, Vol. 34, No. 2, pp. 217–231.

Palmer, M. A.; Bernhardt, E. S.; Schlesinger, W. H.; Eshleman, K. N.; Foufoula-Georgiou, E.; Hendryx, M. S.; Lemly, A. D.; Likens, G. E.; Loucks, O. L.; Power, M. E.; White, P. S.; and Wilcock, P. R., 2010, Mountaintop mining consequences: *Science*, Vol. 327, No. 5962, pp. 148–149.

Rafique, M. U.; Zhu, J.; and Jacobs, N., 2022, Automatic segmentation of sinkholes using a convolutional neural network: *Earth and Space Science*, Vol. 9, No. 2, p. e2021EA002195.

Reed, M. and Kite, S., 2020, Peripheral gully and landslide erosion on an extreme anthropogenic landscape produced by mountaintop removal coal mining: *Earth Surface Processes and Landforms*, Vol. 45, No. 9, pp. 2078–2090.

RODRIGUE, J.; BURGER, J.; AND ODERWALD, R., 2002, Forest productivity and commercial value of pre-law reclaimed mined land in the eastern United States: *Northern Journal of Applied Forestry*, Vol. 19, No. 3, pp. 106–114.

ROEN, J. B.; KENT, B. H.; AND SCHWEINFURTH, S. P., 1968, *Geologic Map of the Monongahela Quadrangle, Southwestern Pennsylvania*: U.S. Geological Survey Geologic Quadrangle 743.

ROSS, M. R.; MCGLYNN, B. L.; AND BERNHARDT, E. S., 2016, Deep impact: Effects of mountaintop mining on surface topography, bedrock structure, and downstream waters: *Environmental Science & Technology*, Vol. 50, No. 4, pp. 2064–2074.

RUPPERT, L. F. AND RICE, C. L., 2000, *Coal Resource Assessment Methodology and Geology of the Northern and Central Appalachian Basin Coal Regions*: U.S. Geological Survey Professional Paper 1625-C, Chapter B–.

SENA, K.; FRANKLIN, J. A.; SWAB, R. M.; AND HALL, S. L., 2021, Plant communities on Appalachian mined lands. In Zipper, C. E. and Skousen, J. (Editors), *Appalachia's Coal-Mined Landscapes: Resources and Communities in a New Energy Era*: Springer, Cham, Switzerland, pp. 111–134.

SHOBE, C. M.; BOWER, S. J.; MAXWELL, A. E.; GLADE, R. C.; AND SAMASSI, N. M., 2024, The uncertain future of mountaintop-removal-mined landscapes 1: How mining changes erosion processes and variables: *Geomorphology*, Vol. 445, p. 108984.

SIMATE, G. S. AND NDLOVU, S., 2014, Acid mine drainage: Challenges and opportunities: *Journal of Environmental Chemical Engineering*, Vol. 2, No. 3, pp. 1785–1803.

SINGH, S.; VINOD KUMAR, K.; AND JAGANNADHA RAO, M., 2020, Utilization of LiDAR DTM for systematic improvement in mapping and classification of coastal micro-geomorphology: *Journal of the Indian Society of Remote Sensing*, Vol. 48, pp. 805–816.

SKOUSEN, J. G.; SEXSTONE, A.; AND ZIEMKIEWICZ, P. F., 2000, Acid mine drainage control and treatment. In Barnhisel, R. I.; Darmody, R. G.; and Daniels, W. L. (Editors), Reclamation of Drastically Disturbed Lands: American Society of Agronomy, Crop Science Society of America, and Soil Science Society of America, Madison, WI, Agronomy Vol. 41, pp. 131–168.

SOUTHWORTH, C. S., 1988, Large Quaternary landslides in the central Appalachian Valley and ridge province near Petersburg, West Virginia: *Geomorphology*, Vol. 1, No. 4, pp. 317–329.

STAGE, A. R., 1976, An expression for the effect of aspect, slope, and habitat type on tree growth: *Forest Science*, Vol. 22, No. 4, pp. 457–460.

STRAUSBAUGH, P. D. AND CORE, E. L., 1978, *Flora of West Virginia*: Seneca Press, Grantsville, WV.

ŠTULAR, B.; LOZIé, E.; AND EICHERT, S., 2021, Airborne LiDAR-derived digital elevation model for archaeology: *Remote Sensing*, Vol. 13, No. 9, p. 1855.

U.S. GEOLOGICAL SURVEY (USGS), 2023, *Prospect- and Mine-Related Features from U.S. Geological Survey 7.5- and 15-Minute Topographic Quadrangle Maps of the United States* (ver. 10.0, May 2023): Electronic document, available at https://www.sciencebase.gov/catalog/item/5a1492c3e4b09fc93dcfd574

U.S. GEOLOGICAL SURVEY (USGS), 2024, *Landslide Basics*: Electronic document, available at https://www.usgs.gov/programs/landslide-hazards/landslide-basics

WILKINSON, B. H., 2005, Humans as geologic agents: A deep-time perspective: *Geology*, Vol. 33, No. 3, pp. 161–164.

WOOTEN, R. M.; WITT, A. C.; MINIAT, C. F.; HALES, T. C.; AND ALDRED, J. L., 2016, Frequency and magnitude of selected historical landslide events in the southern Appalachian Highlands of North Carolina and Virginia: Relationships to rainfall, geological and ecohydrological controls, and effects. In Greenberg, C. H. and Collins, B. S. (Editors), *Natural Disturbances and Historic Range of Variation: Type, Frequency, Severity, and Post-Disturbance Structure in Central Hardwood Forests USA*: Springer, Cham, Switzerland, Managing Forest Ecosystems Vol. 32, pp. 203–262.

WVGES::INTERACTIVE COAL BED MAPPING PROJECT (CBMP), 2024. Interactive Coal Bed Mapping Project: Electronic document, available at https://www.wvgs.wvnet.edu/www/coal/cbmp/coalims.html

YONK, R. M.; SMITH, J. T.; AND WARDLE, A. R., 2019, Exploring the policy implications of the Surface Mining Control and Reclamation Act: *Resources*, Vol. 8, No. 1, p. 25.

ZIPPER, C. E.; BURGER, J. A.; SKOUSEN, J. G.; ANGEL, P. N.; BARTON, C. D.; DAVIS, V.; AND FRANKLIN, J. A., 2011, Restoring forests and associated ecosystem services on Appalachian coal surface mines: *Environmental Management*, Vol. 47, pp. 751–765.

ZIPPER, C. E.; DANIELS, W. L.; AND BELL, J. C., 1989, The practice of "approximate original contour" in the central Appalachians. II. Economic and environmental consequences of an alternative: *Landscape and Urban Planning*, Vol. 18, No. 2, pp. 139–152.

ZIPPER, C. E. AND SKOUSEN, J., 2021, Coal's legacy in Appalachia: Lands, waters, and people: *The Extractive Industries and Society*, Vol. 8, No. 4, p. 100990.